Observation of the very rare $\Sigma^+ \to p\mu^+\mu^-$ decay

R. Aaij *et al.*[*]
(LHCb Collaboration)

(Received 9 April 2025; accepted 2 June 2025; published 29 July 2025)

The first observation of the $\Sigma^+ \to p\mu^+\mu^-$ decay is reported with high significance using proton-proton collision data, corresponding to an integrated luminosity of 5.4 fb^{-1}, collected with the LHCb detector at a center-of-mass energy of 13 TeV. A yield of 237 ± 16 $\Sigma^+ \to p\mu^+\mu^-$ decays is obtained, where the uncertainty is statistical only. A branching fraction of $(1.08 \pm 0.17) \times 10^{-8}$ is measured, where the uncertainty includes statistical and systematic sources. No evidence of resonant structures is found in the dimuon invariant-mass distribution. All results are compatible with standard model expectations. This represents the rarest decay of a baryon ever observed.

DOI: 10.1103/r3v2-kmmp

The $\Sigma^+ \to p\mu^+\mu^-$ decay is a flavor-changing neutral-current (FCNC) process that is allowed only at loop level within the standard model (SM). The decay rate could be significantly modified by the presence of new physics (NP) beyond the SM effects. Short-distance contributions in the SM arise from box, Z, and electromagnetic-penguin processes, whose combined branching fraction is predicted to be $\mathcal{O}(10^{-12})$ [1]. While this is significantly smaller than the predicted long-distance contribution, it is worth noting that NP contributions are expected to manifest at short distance [2–4], potentially modifying the expected decay rate. The long-distance SM contribution is calculated from weak nonleptonic decays $\Sigma^+ \to (N\pi)^+$ and the subsequent reactions $(N\pi)^+ \to p\gamma^{(*)}$ (the inclusion of charge-conjugated processes is implied throughout this Letter), where N represents either a proton, p, or a neutron, n, and γ^* is a virtual photon. The branching fraction prediction contains an inherent eight-fold ambiguity due to the presence of four complex form factors studied in both relativistic and heavy-baryon chiral perturbation theory (χPT). A unitarity argument determines their imaginary parts [1–3,5–7], while the real components are predicted from the measured $\Sigma^+ \to p\gamma$ decay rate [8], which is responsible for a remaining four-fold degeneracy in each χPT approach. The most recent theoretical predictions for the branching fraction $\mathcal{B}(\Sigma^+ \to p\mu^+\mu^-)$ lie within the range $[1.2, 7.8] \times 10^{-8}$ [3]. Progress has also been made toward a lattice calculation of this branching fraction [9,10].

Evidence for this channel was first found by the HyperCP experiment with a measured branching fraction of $\mathcal{B}(\Sigma^+ \to p\mu^+\mu^-) = (8.6^{+6.6}_{-5.4} \pm 5.5) \times 10^{-8}$ [11], compatible with all SM predictions. Note that the measurement was based on three observed candidates with nearly identical dimuon invariant mass, close to the kinematic limit, suggesting an unexpected hint of structure with mass $m_{X^0} = 214.3 \pm 0.5$ MeV/c^2. If confirmed, this would have pointed toward the decay of an intermediate particle into two muons, i.e., a $\Sigma^+ \to pX^0(\to \mu^+\mu^-)$ decay. This result attracted significant theoretical attention attempting to explain the origin of this hypothetical state [12–22]. In general, a pseudoscalar particle is favored over a scalar state, with a lifetime in the order of 10^{-14} s estimated for the former. Considerable experimental efforts have been made in order to search for this particle in other experiments and decay modes [23–34]. The first search using $\Sigma^+ \to p\mu^+\mu^-$ decays since the HyperCP evidence was performed by LHCb with Run 1 proton-proton (pp) collision data [35], corresponding to an integrated luminosity of 3 fb^{-1} collected at a center-of-mass energy $\sqrt{s} = 7$ TeV. An excess of $10.2^{+3.9}_{-3.5}$ events was observed with a significance of 4.1 standard deviations (σ), corresponding to a branching fraction of $\mathcal{B}(\Sigma^+ \to p\mu^+\mu^-) = (2.2^{+1.8}_{-1.3}) \times 10^{-8}$, compatible with all SM predictions. The background-subtracted dimuon invariant-mass distribution was consistent with that of a phase-space (PHSP) simulation, leading to an upper limit of $\mathcal{B}(\Sigma^+ \to pX^0(\to \mu\mu)) < 1.4 \times 10^{-8}$ at the 90% confidence level for a hypothetical X^0 particle, which disfavors the central value determined by the HyperCP collaboration.

This Letter presents the first observation of the $\Sigma^+ \to p\mu^+\mu^-$ decay. This analysis is performed with pp collision data recorded by the LHCb experiment in 2016–2018 (Run 2) at $\sqrt{s} = 13$ TeV, corresponding to an integrated luminosity of 5.4 fb^{-1}. A measurement of the

[*]Full author list given at the end of the Letter.

$\Sigma^+ \to p\mu^+\mu^-$ branching fraction is reported, using the $\Sigma^+ \to p\pi^0$ decay as normalisation channel. The dimuon invariant-mass distribution for signal decays is also presented. This analysis follows a similar strategy to that performed using Run 1 data [35], with several improvements implemented, namely more efficient particle identification (PID), larger simulated samples and, most importantly, additional trigger selections that increase the signal efficiency by an order of magnitude, in addition to yield enhancements that naturally accompany increases in cross section and luminosity. In order to avoid experimenter's bias, the dimuon invariant-mass distribution was not examined and a random factor was kept in the branching fraction normalization until the full analysis was finalized.

The LHCb detector is a single-arm forward spectrometer covering the pseudorapidity range $2 < \eta < 5$, described in detail in Refs. [36,37]. Due to its lifetime of $(8.018 \pm 0.026) \times 10^{-11}$ s [38], the Σ^+ baryon can decay both inside the vertex detector, such that all decay products are reconstructed using the full tracking system (long tracks), or downstream of the vertex detector (downstream tracks). In this analysis, only long tracks are used. The short lifetime estimated for the X^0 particle would result in prompt signal production; hence, no attempt is made to distinguish the dimuon origin vertex from the decay vertex of the Σ^+ baryon in this search.

The online event selection is performed by a trigger consisting of a hardware stage, using information from the calorimeter and muon systems, followed by two software stages, where a full event reconstruction is performed. Since 2016, two inclusive dimuon trigger selections have been added at the two software trigger stages, specifically designed to retain low transverse-momentum, p_{T}, track combinations while remaining within the strict processing time constraints imposed for the software trigger. In these selections, muon tracks are required to be inconsistent with originating from any primary vertex (PV) and to have PID information consistent with their mass hypothesis. More details can be found in Refs. [39,40]. In addition, an exclusive trigger selection has been introduced for the $\Sigma^+ \to p\mu^+\mu^-$ decay channel. Candidate Σ^+ baryons are formed from combinations of a pair of oppositely charged muons and one proton candidate that are inconsistent with originating from any PV, with a good track-fit quality, and which form a good-quality vertex [41]. The Σ^+ candidate is required to have $p_{\mathrm{T}} > 500$ MeV/c, be consistent with originating from a PV, and to have a significant flight distance. The $\Sigma^+ \to p\pi^0$ decay, used as normalization channel, is selected from a well-identified proton track and a π^0 candidate reconstructed in the two-photon final state from two clusters in the calorimeter. For events with multiple candidates, all are accepted.

Given the large production rate of Σ^+ baryons in pp collisions, the present search is conducted also including data selected at one or more trigger stages by other particles in the event. In the offline processing phase, trigger decisions are associated with reconstructed candidates. A trigger decision can thus be ascribed to the reconstructed candidate, the rest of the event, or a combination of both. In the triggered on signal (TOS) sample the signal decay products are required to pass the muon or the hadron triggers, and the proton from $\Sigma^+ \to p\pi^0$ decays is required to pass the hadron trigger. In the triggered independently of signal (TIS) sample, both channels are selected in events where their decay products are not necessary for the trigger decision. Candidates from the two samples are selected together, but the measurement of the signal branching fraction is performed separately for the TIS and TOS samples. At the software trigger level, the signal selection already described is maintained for both samples. The normalization channel is selected at the first software level by requiring a high p_{T} hadron, while a minimum-bias selection, with a fixed scale factor of 10^{-4} to limit its rate, is applied at the second software level.

Simulated samples are used to optimize the selection criteria, parametrize invariant-mass distributions, and characterize the detector resolution and efficiencies. These samples are generated with the software described in Refs. [42–47]. The signal $\Sigma^+ \to p\mu^+\mu^-$ decay is generated according to a PHSP model and weighted to reproduce the SM dimuon invariant-mass predicted spectrum [2,3]. Simulated samples are weighted to reproduce the multiplicity distribution observed in data.

Two sources of background remain after the offline selection: the combinatorial background, composed from random associations of tracks present in the event, and the Λ background, consisting of genuine $\Lambda \to p\pi^-$ decays where the pion is misidentified as a muon, combined with a third unrelated track identified as a muon. No other kinds of background contribute, owing mainly to the very small energy of 39.8 MeV available in the $\Sigma^+ \to p\mu^+\mu^-$ reaction. Misidentified decays from other hadrons also do not contribute. Background from four- or more-body final states with unreconstructed particles could contribute, but would not peak in the $m_{p\mu^+\mu^-}$ distribution and thus is included in the combinatorial background. Finally, background including duplicate tracks from the same particle hits is rejected offline with a requirement on the minimum angle between each pair of tracks. Additional details on the background sources are reported in Appendix A.

To further reduce the background, a multivariate classifier is devised based on a Boosted Decision Tree (BDT) algorithm [48,49] implemented in the TMVA toolkit [50,51]. This BDT algorithm combines different kinematic and geometric variables. The BDT is trained using the signal simulated sample and the data sidebands as a proxy for combinatorial background considering candidates in the mass range $m_{p\mu^+\mu^-} < 1173$ MeV/c^2 or $1205 < m_{p\mu^+\mu^-} < 1400$ MeV/c^2. Under the $p\pi^-$ hypothesis, a veto on the

$p\mu^-$ mass is applied in both samples around the known Λ mass value [38] (Λ veto) to enforce training against combinatorial background only. To avoid overtraining, the k-folding technique [52], with $k = 9$, is applied. The BDT output ranges from zero, for background-like candidates, to unity, for signal-like candidates; the corresponding distributions for signal simulation and data are shown in Supplemental Material [53]. The data is divided into a sample with the Λ veto and its complementary sample, consisting mostly of the Λ background, where the BDT distribution is seen to be very similar for both background sources. The same BDT classifier is applied to a sample of "same-sign" $\Sigma^+ \to \bar{p}\mu^+\mu^+$ candidates in data, where a signal would have to violate lepton-number conservation, verifying that fake structures in the background are not created in either the $m_{p\mu^+\mu^-}$ or $m_{\mu^+\mu^-}$ distributions.

The final selection is based on the BDT output, the muon and proton particle-identification variables [54], and the width of the Λ veto window. Criteria on these variables are optimised on a four-dimensional grid to give the largest significance, defined as $N_S/\sqrt{N_S + N_B}$, where N_S is the expected signal and N_B the expected background yield. The N_S estimate is based on a preliminary fit to data after tight selection criteria are applied along with the signal efficiency obtained from simulation. The N_B estimate is the sum of two contributions: one obtained from a fit to the $m_{p\mu^+\mu^-}$ sidebands for the combinatorial background; and another to estimate the residual Λ background based on a fit to the $m_{p\pi^-}$ distribution without the Λ veto (± 10 MeV$/c^2$ around the known Λ mass [38]). The optimised requirements on the BDT output, particle identification and Λ veto are applied equally to the TIS and TOS samples.

The $m_{p\mu^+\mu^-}$ distribution for candidates satisfying the final selection criteria is shown in Fig. 1, in which a clear peak at the Σ^+ mass is observed with a small residual background. An extended unbinned maximum-likelihood fit [55] is performed to the selected candidates. The signal component is described by a Hypatia function [56], with the z parameter fixed to zero. The remaining parameters are obtained from a fit to the simulated sample and fixed in the fit to data, while the peak position and resolution parameters are left free to vary. The background is described by a modified Argus function [57], where the threshold parameter is fixed to the sum of the final-state masses and the remaining parameters are free to vary. The data and the result of the fit are shown in Fig. 1; a signal yield of $N_{\Sigma^+\to p\mu^+\mu^-} = 237 \pm 16$ is obtained, where the uncertainty is statistical only. This result constitutes the first observation of the $\Sigma^+ \to p\mu^+\mu^-$ decay, obtained with overwhelming significance. The fit to data is repeated, releasing all parameters of the signal function that are fixed from simulation in the baseline model. The variation of the signal yield is negligible, hence no systematic uncertainty is assigned. A similar amount of Σ^+ and $\bar{\Sigma}^-$ decays are seen in the sample.

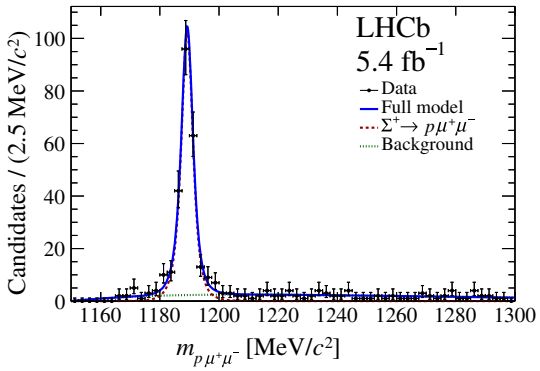

FIG. 1. Distribution of the invariant mass of $\Sigma^+ \to p\mu^+\mu^-$ candidates in a restricted mass range with the result of the extended unbinned maximum-likelihood fit also shown (blue solid line). The signal (red dashed line) and background (green dotted line) components are also illustrated. The full range is shown in Supplemental Material [53].

The distribution of the dimuon invariant mass is shown for data in Fig. 2 after background subtraction. The background is subtracted using per-event signal weights derived with the *sPlot* method [58] using $m_{p\mu^+\mu^-}$ as the discriminant variable. The $m_{p\mu^+\mu^-}$ and $m_{\mu^+\mu^-}$ variables are found to be uncorrelated aside from the higher border of the kinematics space. A consistent distribution is obtained when performing the unbinned maximum-likelihood fit described earlier in intervals of the dimuon invariant mass. No significant peaking structures are visible in the data distribution. The data is compared to the distribution in simulation with the PHSP model and with the SM weighted distribution, with theoretical uncertainty due to the mentioned parametric ambiguity shown as a red band in Fig. 2. When comparing the data to this SM simulation, rather good agreement is achieved in the full range, with a

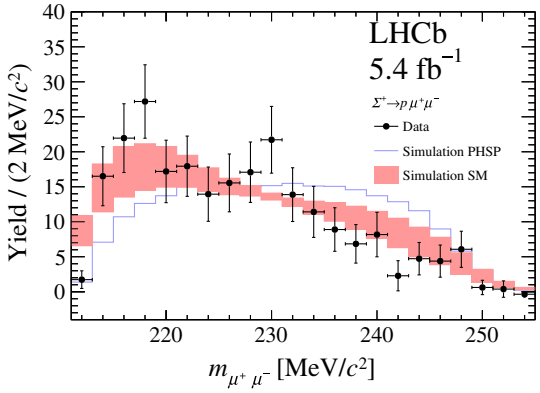

FIG. 2. Distribution of background-subtracted dimuon invariant mass for $\Sigma^+ \to p\mu^+\mu^-$ candidates in data compared with simulation. LHCb PHSP simulation is shown as is (blue line), and weighted according to the SM amplitude [2,3] (red band). Note: the distributions in this figure are not corrected for the efficiencies.

qualitative preference for the lowest predicted degenerate branching fraction [3].

A scan for possible resonant structure in the dimuon invariant mass is performed by selecting candidates in the $p\mu^+\mu^-$ invariant mass within twice the signal resolution of the known Σ^+ mass, using the same method as in the Run 1 analysis [35], and detailed in Appendix C. Steps of half the resolution on the dimuon invariant mass, $\sigma(m_{\mu^+\mu^-})$, are considered in this scan, following the method outlined in Ref. [59]. The value of $\sigma(m_{\mu^+\mu^-})$ varies in the range $[0.5, 2.0]$ MeV$/c^2$ depending on the dimuon invariant mass. For each step, the putative signal is estimated in a window of $\pm 1.5 \times \sigma(m_{\mu^+\mu^-})$ around the considered particle mass, while the background is estimated from the lower and upper mass sidebands contained in the range $[1.5, 4.0] \times \sigma(m_{\mu^+\mu^-})$ for the same mass. Only one of the two sidebands is considered when the other is outside the allowed kinematic range. The local p-value of the background-only hypothesis is shown in Appendix C as a function of the dimuon invariant mass. No significant signal is found; the most significant point occurs at 247.06 MeV$/c^2$, with a p value of 3.5%. When considering a putative candidate with a mass $m_{X^0} = 214.3$ MeV$/c^2$ [11], the fractional contribution to all candidates in the $p\mu^+\mu^-$ signal mass window is 5% and the difference with respect to the expected background from the $m_{\mu^+\mu^-}$ sidebands (i.e., nonresonant) is -1 candidates.

The $\Sigma^+ \to p\mu^+\mu^-$ decay is normalized to the $\Sigma^+ \to p\pi^0$ decay in order to measure its branching fraction as

$$\mathcal{B}(\Sigma^+ \to p\mu^+\mu^-) = \frac{\varepsilon_{\rm Norm}}{\varepsilon_{\rm Sig}} \frac{N_{\rm Sig}}{N_{\rm Norm}} \mathcal{B}(\Sigma^+ \to p\pi^0) = \alpha N_{\rm Sig}, \tag{1}$$

where ε and N are the efficiency and yield of the indicated channel, $\mathcal{B}(\Sigma^+ \to p\pi^0) = (51.57 \pm 0.30)\%$ [38], and α is the single event sensitivity. The efficiencies in Eq. (1) are factorized into different categories for ease of estimation and each is evaluated with respect to the previous steps: detector acceptance, reconstruction and selection, PID, and trigger, and the yields are estimated from fits to their respective innvariant-mass distributions as described later.

The acceptance, reconstruction, and selection efficiencies are obtained from simulation. Possible residual differences between data and simulation in the tracking efficiencies are determined using control data samples [60]. The uncertainty on the theoretical spectrum is propagated to the efficiency as a systematic uncertainty amounting to 2.5%. The PID efficiencies are determined from data using samples of kinematically identified charged particles from $B^+ \to J/\psi K^+$ decays for the muons, and $\Lambda \to p\pi^-$ decays for the protons [54]. Systematic uncertainties of about 1% and 5% are associated with the PID calibration of muons and protons, respectively. Tracking efficiencies are determined in bins of p and η and compared to those from simulation. The weighted average correction is calculated and applied to signal and normalization simulated samples. A total systematic uncertainty of about 5% is associated with this calibration. The π^0 reconstruction efficiency is calibrated using $B^+ \to J/\psi K^{*+}(\to K^+\pi^0)$ and $B^+ \to J/\psi K^+$ decays [61–64], for which a systematic uncertainty of 7%, mostly due to the branching fractions of the calibration channels, is assigned.

The hardware hadron trigger efficiencies, for both signal and normalization channels, are evaluated with two methods: the TISTOS method [65,66] in data, using the normalization channel, and independent estimates based on control samples in data, obtained with similar methods as in Ref. [67]; from the comparison of the two methods a 12% relative systematic uncertainty is assigned. The hardware muon trigger efficiencies for the signal are evaluated similarly to Refs. [68,69]. There, given the lack of other low-$p_{\rm T}$ calibration channels, the $K^0_{\rm S} \to \pi\mu\nu$ channel was used, with the pion decaying in flight into a muon. In this analysis, the $K^+ \to \pi^+\pi^-\pi^+$ channel is used, where two opposite-sign pions are identified as muons. Following Refs. [68,69], a systematic uncertainty is assigned to the TOS sample which includes data-simulation agreement and the method verification, and amounts to 22%. The efficiency of the TIS hardware trigger category is estimated with $\Sigma^+ \to p\pi^0$ decays in data with the TISTOS method and corrected for the residual correlation with the decay kinematics. A systematic uncertainty of 6% is assigned.

The efficiency of the requirement on the BDT output is calibrated directly on $\Sigma^+ \to p\mu^+\mu^-$ decays by comparing the data and simulation distribution above the chosen value. To account for the small disagreement between data and simulation, the data distribution is extrapolated to lower BDT output values to obtain an efficiency correction for the simulation. The distribution is well described by a first-order polynomial, however a second-order is also employed with the difference assigned as a systematic uncertainty.

The yield of the $\Sigma^+ \to p\pi^0$ channel is obtained through an unbinned maximum-likelihood fit to the distribution of the corrected mass, defined as $m_{\rm Corr} \equiv m_{p\gamma\gamma} - m_{\gamma\gamma} + m^{\rm PDG}_{\pi^0}$. Here, $m_{p\gamma\gamma}$ is the invariant mass of the proton and two photons, $m_{\gamma\gamma}$ that of the two photons from which the π^0 is reconstructed, and $m^{\rm PDG}_{\pi^0}$ is the known π^0 mass [38]. The $\Sigma^+ \to p\pi^0$ probability distribution function is composed of the sum of a Gaussian and a crystal ball function [70], with power-law tails on both sides. The background component is described by a Chebyshev second-degree polynomial of the first kind. The $\Sigma^+ \to p\pi^0$ tail parameters are obtained from simulation, while the remaining parameters are free in the fit. The distribution of $m_{\rm Corr}$ is shown in Fig. 3; a total of $(6.13 \pm 0.10) \times 10^3$ and $(4.746 \pm 0.031) \times 10^4$ $\Sigma^+ \to p\pi^0$ candidates is obtained for the TOS and TIS samples, respectively. Studies of the $\Sigma^+ \to p\pi^0$ yield using

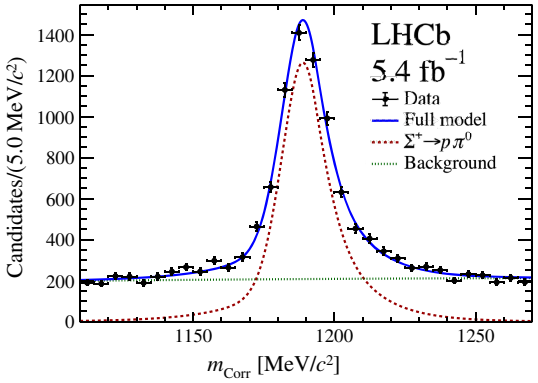

FIG. 3. Distribution of the corrected mass for $\Sigma^+ \to p\pi^0$ decays in data for the TOS sample with the result of an extended unbinned maximum-likelihood fit (blue solid line). The $\Sigma^+ \to p\pi^0$ (red dashed line) and background (green dotted line) components are also shown.

alternative background parametrisations show variations that are negligible with respect to the statistical uncertainty, hence no additional systematic uncertainty is associated to this fit. With Eq. (1), the single-event sensitivities of the two samples are $\alpha_{\rm TOS} = (1.65^{+0.09\ +0.41}_{-0.16\ -0.41}) \times 10^{-10}$ and $\alpha_{\rm TIS} = (6.81^{+0.29\ +0.85}_{-0.25\ -0.85}) \times 10^{-11}$, respectively, where the first uncertainty is statistical and the second systematic.

The fit to the $\Sigma^+ \to p\mu^+\mu^-$ invariant-mass distribution is repeated separately for the TOS and TIS samples, with total yields of 96 ± 10 and 154 ± 13, respectively. These correspond to the measured branching fractions $\mathcal{B}_{\rm TOS} = (1.59^{+0.19\ +0.40}_{-0.23\ -0.40}) \times 10^{-8}$ and $\mathcal{B}_{\rm TIS} = (1.05^{+0.10\ +0.13}_{-0.10\ -0.13}) \times 10^{-8}$, respectively, where the first uncertainty is statistical and the second systematic. The two branching fractions are then combined as a weighted average, factorising common efficiencies to take correlations into account. The resulting branching fraction is

$$\mathcal{B}(\Sigma^+ \to p\mu^+\mu^-) = (1.08 \pm 0.17) \times 10^{-8},$$

where the uncertainty includes statistical and systematic sources. This result is in agreement with the SM predictions [1–3]. The combination with the value obtained in Run 1 [35], which has a large uncertainty, results in $\mathcal{B}(\Sigma^+ \to p\mu^+\mu^-) = (1.09 \pm 0.17) \times 10^{-8}$.

In summary, the $\Sigma^+ \to p\mu^+\mu^-$ decay is observed with very high significance in data collected in Run 2 by the LHCb experiment in pp collisions, with a yield of $N_{\Sigma^+\to p\mu^+\mu^-} = 237 \pm 16$. No structure is seen in the dimuon invariant-mass distribution, which is compatible with expectations from the SM. The $\Sigma^+ \to p\mu^+\mu^-$ branching fraction, when combined with the Run 1 result, is measured to be

$$\mathcal{B}(\Sigma^+ \to p\mu^+\mu^-) = (1.09 \pm 0.17) \times 10^{-8},$$

which is compatible with the SM and represents the rarest baryon decay ever observed. From the combined experimental and theoretical z scores, this result favors the lowest predicted degenerate branching fraction [3], which is also qualitatively favored by the structure measured in the $m_{\mu^+\mu^-}$ distribution. Comparing the measured branching fraction with the eight theoretical predictions [3], the next largest is disfavored by at least 3.7σ, while the remaining two are rejected at over 6.1σ. This comparison also shows that, in general, heavy-baryon χPT predictions are disfavored by at least 3.1σ compared to relativistic χPT predictions.

With the collected signal yield, a measurement of additional observables such as the differential branching fraction, charge-parity symmetry violation, and forward-backward asymmetries is envisaged and left for a future publication.

Acknowledgments—We express our gratitude to our colleagues in the CERN accelerator departments for the excellent performance of the LHC. We thank the technical and administrative staff at the LHCb institutes. We acknowledge support from CERN and from the national agencies: ARC (Australia); CAPES, CNPq, FAPERJ, and FINEP (Brazil); MOST and NSFC (China); CNRS/IN2P3 (France); BMBF, DFG, and MPG (Germany); INFN (Italy); NWO (Netherlands); MNiSW and NCN (Poland); MCID/IFA (Romania); MICIU and AEI (Spain); SNSF and SER (Switzerland); NASU (Ukraine); STFC (United Kingdom); DOE NP and NSF (USA). We acknowledge the computing resources that are provided by ARDC (Australia), Centro Brasileiro de Pesquisas Físicas (CBPF) (Brazil), CERN, IHEP and LZU (China), IN2P3 (France), KIT and DESY (Germany), INFN (Italy), SURF (Netherlands), Polish WLCG (Poland), IFIN-HH (Romania), PIC (Spain), CSCS (Switzerland), and GridPP (United Kingdom). We are indebted to the communities behind the multiple open-source software packages on which we depend. Individual groups or members have received support from Key Research Program of Frontier Sciences of CAS, CAS PIFI, CAS CCEPP, Fundamental Research Funds for the Central Universities, and Sci. & Tech. Program of Guangzhou (China); Minciencias (Colombia); EPLANET, Marie Skłodowska-Curie Actions, ERC, and NextGenerationEU (European Union); A*MIDEX, ANR, IPhU and Labex P2IO, and Région Auvergne-Rhône-Alpes (France); Alexander-von-Humboldt Foundation (Germany); ICSC (Italy); Severo Ochoa and María de Maeztu Units of Excellence, GVA, XuntaGal, GENCAT, InTalent-Inditex and Prog. Atracción Talento CM (Spain); SRC (Sweden); the Leverhulme Trust, the Royal Society and UKRI (United Kingdom).

Data availability—The data that support the findings of this article are openly available [71], embargo periods may apply

[1] X.-G. He, J. Tandean, and G. Valencia, The decay $\Sigma^+ \to p\ell^+\ell^-$ within the Standard Model, Phys. Rev. D **72**, 074003 (2005).

[2] X.-G. He, J. Tandean, and G. Valencia, Decay rate and asymmetries of $\Sigma^+ \to p\mu^+\mu^-$, J. High Energy Phys. 10 (2018) 040.

[3] A. Roy, J. Tandean, and G. Valencia, $\Sigma^+ \to p\ell^+\ell^-$ decays within the Standard Model and beyond, Phys. Rev. D **111**, 013003 (2025).

[4] L.-S. Geng, J. M. Camalich, and R.-X. Shi, New physics in $s \to d$ semileptonic transitions: Rare hyperon vs. kaon decays, J. High Energy Phys. 02 (2022) 178.

[5] D. Corrigan and N. N. Trofimenkoff, Predictions for the decays $\Sigma^+ \to p\mu^+\mu^-$ and $\Sigma^+ \to pe^+e^-$, Nucl. Phys. **B40**, 98 (1972).

[6] L. Bergstrom, R. Safadi, and P. Singer, Phenomenology of $\Sigma^+ \to p\ell^+\ell^-$ and the structure of the weak nonleptonic Hamiltonian, Z. Phys. C **37**, 281 (1988).

[7] I. V. Lyagin and E. K. Ginzburg, On $\Sigma^+ \to pe^+e^-$ and $\Sigma^+ \to p\mu^+\mu^-$ decays, Sov. Phys. JETP **14**, 653 (1962).

[8] M. Ablikim *et al.* (BESIII Collaboration), Precision measurement of the decay $\Sigma^+ \to p\gamma$ in the process $J/\psi \to \Sigma^+\bar{\Sigma}^-$, Phys. Rev. Lett. **130**, 211901 (2023).

[9] F. Erben *et al.*, Prospects for a lattice calculation of the rare decay $\Sigma^+ \to p\ell^+\ell^-$, J. High Energy Phys. 04 (2023) 108.

[10] F. Erben *et al.*, Progress on the exploratory calculation of the rare hyperon decay $\Sigma^+ \to p\ell^+\ell^-$, Proc. Sci., LATTICE2022 (**2023**) 315 [arXiv:2212.09595].

[11] H. Park *et al.* (HyperCP Collaboration), Evidence for the decay $\Sigma^+ \to p\mu^+\mu^-$, Phys. Rev. Lett. **94**, 021801 (2005).

[12] X.-G. He, J. Tandean, and G. Valencia, Does the HyperCP evidence for the decay $\Sigma^+ \to p\mu^+\mu^-$ indicate a light pseudoscalar Higgs boson?, Phys. Rev. Lett. **98**, 081802 (2007).

[13] X.-G. He, J. Tandean, and G. Valencia, Light Higgs production in hyperon decay, Phys. Rev. D **74**, 115015 (2006).

[14] D. S. Gorbunov and V. A. Rubakov, On sgoldstino interpretation of HyperCP events, Phys. Rev. D **73**, 035002 (2006).

[15] S. V. Demidov and D. S. Gorbunov, More about the sgoldstino interpretation of HyperCP events, JETP Lett. **84** (2007) 479,

[16] X.-G. He, J. Tandean, and G. Valencia, Implications of a new particle from the HyperCP data on $\Sigma^+ \to p\mu^+\mu^-$, Phys. Lett. B **631**, 100 (2005).

[17] C. Q. Geng and Y. K. Hsiao, Constraints on the new particle in $\Sigma^+ \to p\mu^+\mu^-$, Phys. Lett. B **632**, 215 (2006).

[18] N. G. Deshpande, G. Eilam, and J. Jiang, On the possibility of a new boson X^0 (214-MeV) in $\Sigma^+ \to p\mu^+\mu^-$, Phys. Lett. B **632**, 212 (2006).

[19] C.-H. Chen, C.-Q. Geng, and C.-W. Kao, U-boson and the HyperCP exotic events, Phys. Lett. B **663**, 400 (2008).

[20] G. Xiangdong, C. S. Li, Z. Li, and H. Zhang, Contributions from SUSY-FCNC couplings to the interpretation of the HyperCP events for the decay $\Sigma^+ \to p\mu^+\mu^-$, Eur. Phys. J. C **55**, 317 (2008).

[21] M. L. Mangano and P. Nason, Radiative quarkonium decays and the NMSSM Higgs interpretation of the HyperCP $\Sigma^+ \to p\mu^+\mu^-$ events, Mod. Phys. Lett. A **22**, 1373 (2007).

[22] M. Pospelov, Secluded U(1) below the weak scale, Phys. Rev. D **80**, 095002 (2009).

[23] W. Love *et al.* (CLEO Collaboration), Search for very light CP-odd Higgs boson in radiative decays of Υ (1S), Phys. Rev. Lett. **101**, 151802 (2008).

[24] Y. C. Tung *et al.* (E391a Collaboration), Search for a light pseudoscalar particle in the decay $K_L^0 \to \pi^0\pi^0 X$, Phys. Rev. Lett. **102**, 051802 (2009).

[25] V. M. Abazov *et al.* (D0 Collaboration), Search for next-to-minimal supersymmetric Higgs bosons in the $\mu\mu\tau\tau$ channels using $p\bar{p}$ at $\sqrt{s} = 1.96$ TeV, Phys. Rev. Lett. **103**, 061801 (2009).

[26] B. Aubert *et al.* (*BABAR* Collaboration), Search for dimuon decays of a light scalar boson in radiative transitions $\Upsilon \to \gamma A^0$, Phys. Rev. Lett. **103**, 081803 (2009).

[27] H. J. Hyun *et al.* (Belle Collaboration), Search for a low mass particle decaying into $\mu^+\mu^-$ in $B^0 \to K^{*0}X$ and $B^0 \to \rho^0 X$ at Belle, Phys. Rev. Lett. **105**, 091801 (2010).

[28] E. Abouzaid *et al.* (KTeV Collaboration), Search for the rare decays $K_L \to \pi^0\pi^0\mu^+\mu^-$ and $K_L \to \pi^0\pi^0 X^0 \to \pi^0\pi^0\mu^+\mu^-$, Phys. Rev. Lett. **107**, 201803 (2011).

[29] M. Ablikim *et al.* (BESIII Collaboration), Search for a light Higgs-like boson A^0 in J/ψ radiative decays, Phys. Rev. D **85**, 092012 (2012).

[30] J. P. Lees *et al.* (*BABAR* Collaboration), Search for a dark photon in e^+e^- collisions at *BABAR*, Phys. Rev. Lett. **113**, 201801 (2014).

[31] R. Aaij *et al.* (LHCb Collaboration), Search for rare $B^0_{(s)} \to \mu^+\mu^-\mu^+\mu^-$ decays, Phys. Rev. Lett. **110**, 211801 (2013).

[32] R. Aaij *et al.* (LHCb Collaboration), Search for hidden-sector bosons in $B^0 \to K^{*0}\mu^+\mu^-$ decays, Phys. Rev. Lett. **115**, 161802 (2015).

[33] R. Aaij *et al.* (LHCb Collaboration), Search for long-lived scalar particles in $B^+ \to K^+\chi(\mu^+\mu^-)$ decays, Phys. Rev. D **95**, 071101 (2017).

[34] R. Aaij *et al.* (LHCb Collaboration), Search for dark photons produced in 13 TeV pp collisions, Phys. Rev. Lett. **120**, 061801 (2018).

[35] R. Aaij *et al.* (LHCb Collaboration), Evidence for the rare decay $\Sigma^+ \to p\mu^+\mu^-$, Phys. Rev. Lett. **120**, 221803 (2018).

[36] A. A. Alves Jr. *et al.* (LHCb Collaboration), The LHCb detector at the LHC, J. Instrum. **3**, S08005 (2008).

[37] R. Aaij *et al.* (LHCb Collaboration), LHCb detector performance, Int. J. Mod. Phys. A **30**, 1530022 (2015).

[38] S. Navas *et al.* (Particle Data Group), Review of particle physics, Phys. Rev. D **110**, 030001 (2024).

[39] F. Dettori, D. Martinez Santos, and J. Prisciandaro, Low-p_T dimuon triggers at LHCb in Run 2, Reports No. LHCb-PUB-2017-023, No. CERN-LHCb-PUB-2017-023, CERN, Geneva, 2017, https://cds.cern.ch/record/2297352.

[40] R. Aaij *et al.* (LHCb Collaboration), Design and performance of the LHCb trigger and full real-time reconstruction in Run 2 of the LHC, J. Instrum. **14**, P04013 (2019).

[41] R. Aaij *et al.*, Design and performance of the LHCb trigger and full real-time reconstruction in Run 2 of the LHC, J. Instrum. **14**, P04013 (2019).

[42] T. Sjöstrand, S. Mrenna, and P. Skands, A brief introduction to PYTHIA8.1, Comput. Phys. Commun. **178**, 852 (2008); T. Sjöstrand, S. Mrenna, and P. Skands, PYTHIA6.4 physics and manual, J. High Energy Phys. 05 (2006) 026.

[43] I. Belyaev *et al.*, Handling of the generation of primary events in Gauss, the LHCb simulation framework, J. Phys. Conf. Ser. **331**, 032047 (2011).
[44] D. J. Lange, The EvtGen particle decay simulation package, Nucl. Instrum. Methods Phys. Res., Sect. A **462**, 152 (2001).
[45] N. Davidson, T. Przedzinski, and Z. Was, PHOTOS interface in C++: Technical and physics documentation, Comput. Phys. Commun. **199**, 86 (2016).
[46] J. Allison *et al.* (Geant4 Collaboration), Geant4 developments and applications, IEEE Trans. Nucl. Sci. **53**, 270 (2006); S. Agostinelli *et al.* (Geant4 Collaboration), Geant4: A simulation toolkit, Nucl. Instrum. Methods Phys. Res., Sect. A **506**, 250 (2003).
[47] M. Clemencic *et al.*, The LHCb simulation application, Gauss: Design, evolution and experience, J. Phys. Conf. Ser. **331**, 032023 (2011).
[48] L. Breiman, J. H. Friedman, R. A. Olshen, and C. J. Stone, *Classification and Regression Trees* (Wadsworth international group, Belmont, California, USA, 1984).
[49] Y. Freund and R. E. Schapire, A decision-theoretic generalization of on-line learning and an application to boosting, J. Comput. Syst. Sci. **55**, 119 (1997).
[50] H. Voss, A. Hoecker, J. Stelzer, and F. Tegenfeldt, TMVA—toolkit for multivariate data analysis with ROOT, Proc. Sci., ACAT2007 (**2007**) 040.
[51] A. Hoecker *et al.*, TMVA 4—toolkit for multivariate data analysis with ROOT. users guide, arXiv:physics/0703039.
[52] A. Blum, A. Kalai, and J. Langford, Beating the hold-out: Bounds for k-fold and progressive cross-validation, in *Proceedings of the Twelfth Annual Conference on Computational Learning Theory, COLT '99* (ACM, New York, USA, 1999), p. 203, 10.1145/307400.307439.
[53] See Supplemental Material at http://link.aps.org/supplemental/10.1103/r3v2-kmmp for additional figures.
[54] R. Aaij *et al.*, Selection and processing of calibration samples to measure the particle identification performance of the LHCb experiment in Run 2, Eur. Phys. J. Tech. Instrum. **6**, 1 (2019).
[55] R. J. Barlow, Extended maximum likelihood, Nucl. Instrum. Methods Phys. Res., Sect. A **297**, 496 (1990).
[56] D. Martinez Santos and F. Dupertuis, Mass distributions marginalized over per-event errors, Nucl. Instrum. Methods Phys. Res., Sect. A **764**, 150 (2014).
[57] H. Albrecht *et al.* (ARGUS Collaboration), Search for hadronic $b \to u$ decays, Phys. Lett. B **241**, 278 (1990).
[58] M. Pivk and F. R. Le Diberder, sPlot: A statistical tool to unfold data distributions, Nucl. Instrum. Methods Phys. Res., Sect. A **555**, 356 (2005).
[59] M. Williams, Searching for a particle of unknown mass and lifetime in the presence of an unknown non-monotonic background, J. Instrum. **10**, P06002 (2015).
[60] R. Aaij *et al.* (LHCb Collaboration), Measurement of the track reconstruction efficiency at LHCb, J. Instrum. **10**, P02007 (2015).
[61] R. Aaij *et al.* (LHCb Collaboration), Evidence for the decay $B^0 \to J/\psi\omega$ and measurement of the relative branching fractions of B_s^0 meson decays to $J/\psi\eta$ and $J/\psi\eta'$, Nucl. Phys. **B867**, 547 (2013).
[62] R. Aaij *et al.* (LHCb Collaboration), Observations of $B_s^0 \to \psi(2S)\eta$ and $B_{(s)}^0 \to \psi(2S)\pi^+\pi^-$ decays, Nucl. Phys. **B871**, 403 (2013).
[63] I. M. Belyaev, E. M. Govorkova, V. Y. Egorychev, and D. V. Savrina, Study of π^0/γ reconstruction and selection efficiency in the LHCb experiment, Moscow Univ. Phys. Bull. **70**, 497 (2015).
[64] E. Govorkova, Study of π^0/γ efficiency using B meson decays in the LHCb experiment, Phys. At. Nucl. **79**, 1474 (2016).
[65] R. Aaij *et al.*, The LHCb trigger and its performance in 2011, J. Instrum. **8**, P04022 (2013).
[66] S. Tolk, J. Albrecht, F. Dettori, and A. Pellegrino, Data driven trigger efficiency determination at LHCb, Reports No. LHCb-PUB-2014-039, No. CERN-LHCb-PUB-2014-039, CERN, Geneva, 2014, http://cds.cern.ch/record/1701134.
[67] A. Martin Sanchez, P. Robbe, and M.-H. Schune, Performances of the LHCb L0 calorimeter trigger, Reports No. LHCb-PUB-2011-026, No. CERN-LHCb-PUB-2011-026, CERN, Geneva, 2012, https://cds.cern.ch/record/1407893.
[68] R. Aaij *et al.* (LHCb Collaboration), Constraints on the $K_S^0 \to \mu^+\mu^-$ branching fraction, Phys. Rev. Lett. **125**, 1231801 (2020).
[69] R. Aaij *et al.* (LHCb Collaboration), Search for $K_{S(L)}^0 \to \mu^+\mu^-\mu^+\mu^-$ decays at LHCb, Phys. Rev. D **108**, L031102 (2023).
[70] T. Skwarnicki, A study of the radiative cascade transitions between the Upsilon-prime and Upsilon resonances, Ph.D. thesis, Institute of Nuclear Physics, Krakow, 1986, http://inspirehep.net/record/230779/.
[71] http://cds.cern.ch/record/2929686

End Matter

Appendix A: Additional information on background sources—As described in the main text, no other background source is expected in the selected sample aside from those already included: combinatorial and from misidentified $\Lambda \to p\pi^-$ decays combined with an additional track. The reason only these background sources can contribute is due to the extremely small phase space of the decay. The difference between the Σ^+ mass and the sum of the final-state particles masses is 39.8 MeV/c^2 [38]. This implies that very few decays can mimic this final state at the same mass. In particular, the $\Sigma^+ \to p\pi^+\pi^-$ or $\Sigma^+ \to \Lambda\mu^+\nu_\mu$ decays are forbidden by energy conservation. Given the low energy in the $\Sigma^+ \to p\mu^+\mu^-$ reaction, no background is expected from meson decays. For example, the $K^+ \to \pi^+\pi^-\pi^+$ and $K^+ \to \pi^+\mu^-\mu^+$ decay peaks in the invariant mass of the final state particles, $m_{p\mu^+\mu^-}$, are shifted considerably higher in mass. Higher-mass mesons would be shifted

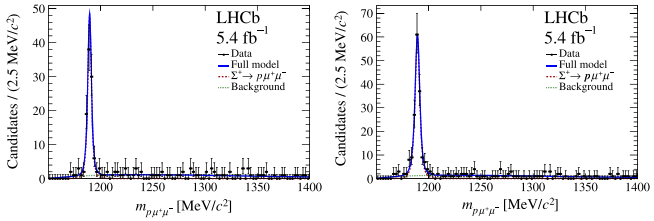

FIG. 4. Distribution of the invariant mass of (left) $\Sigma^+ \to p\mu^+\mu^-$ TOS candidates with the result of an extended unbinned maximum-likelihood fit also shown and (right) corresponding figure for the TIS candidates.

even more. As far as background from baryon decays is concerned, where the final-state proton is correctly identified, the Σ^+ triplet is the lightest state with a significant lifetime, hence all other possible background sources will have a mass that is considerably larger.

Regarding possible residual Λ background, no significant contribution is expected after the full selection including the Λ veto. The distribution of the $p\mu^-$ invariant mass in the $p\pi^-$ hypothesis is shown in the Supplemental Material [53] for $\Sigma^+ \to p\mu^+\mu^-$ candidates in data within a ± 6 MeV$/c^2$ window from the Σ^+ mass peak, without the

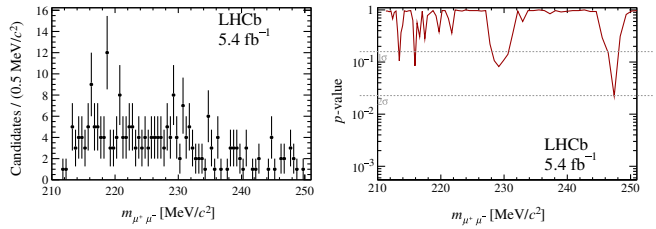

FIG. 5. Distribution of (left) the dimuon invariant mass of $\Sigma^+ \to p\mu^+\mu^-$ decays in a signal region of ± 2 times the resolution on $m_{p\mu^+\mu^-}$, for which no background subtraction is applied. The local p-value (right) is shown in each dimuon invariant-mass window, obtained as described in the text. The horizontal dashed lines correspond to the p values of one and two standard deviations.

Λ veto. The residual background coming from Λ decays outside of the veto represents only a small tail distributed along the $m_{p\mu^+\mu^-}$ mass, taken into account by the combinatorial background.

Appendix B: Fit to the $\Sigma^+ \to p\mu^+\mu^-$ invariant mass—The unbinned maximum-likelihood fit to the $p\mu^+\mu^-$ invariant mass on the data sample divided into TOS and TIS samples is reported in Fig. 4.

Appendix C: Scan for a structure in the dimuon invariant mass—A scan for a possible resonant structure in the dimuon invariant mass is performed as described in the main text. The distribution of $\Sigma^+ \to p\mu^+\mu^-$ candidates in the signal region as a function of the dimuon invariant mass is shown in Fig. 5 (left). The mass resolution $\sigma(m_{\mu^+\mu^-})$ as a function of the dimuon invariant mass is shown in Supplemental Material [53]. The local p value of the background-only hypothesis obtained from the scan for possible structure is shown in Fig. 5 (right) as a function of the dimuon invariant mass.

Appendix D: Fit to the $\Sigma^+ \to p\pi^0$ invariant mass—The extended maximum-likelihood fits to the corrected $p\pi^0$ invariant-mass distribution in data for the TIS and TOS samples are reported in Fig. 6.

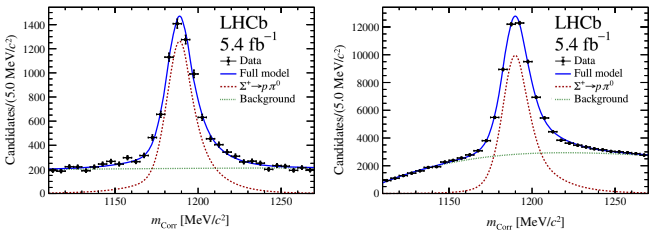

FIG. 6. Distribution of the corrected invariant mass of (left) $p\pi^0$ TOS candidates with the result of an extended maximum-likelihood fit also shown and (right) corresponding figure for the TIS candidates.

R. Aaij,[38] A. S. W. Abdelmotteleb,[57] C. Abellan Beteta,[51] F. Abudinén,[57] T. Ackernley,[61] A. A. Adefisoye,[69] B. Adeva,[47] M. Adinolfi,[55] P. Adlarson,[84] C. Agapopoulou,[14] C. A. Aidala,[86] Z. Ajaltouni,[11] S. Akar,[11] K. Akiba,[38] P. Albicocco,[28] J. Albrecht,[19,b] F. Alessio,[49] Z. Aliouche,[63] P. Alvarez Cartelle,[56] R. Amalric,[16] S. Amato,[3] J. L. Amey,[55] Y. Amhis,[14] L. An,[6] L. Anderlini,[27] M. Andersson,[51] A. Andreianov,[44] P. Andreola,[51] M. Andreotti,[26] D. Andreou,[69] A. Anelli,[31,49,c] D. Ao,[7] F. Archilli,[37,d] M. Argenton,[26] S. Arguedas Cuendis,[9,49] A. Artamonov,[44] M. Artuso,[69] E. Aslanides,[13] R. Ataíde Da Silva,[50] M. Atzeni,[65] B. Audurier,[12] D. Bacher,[64] I. Bachiller Perea,[50] S. Bachmann,[22] M. Bachmayer,[50] J. J. Back,[57] P. Baladron Rodriguez,[47] V. Balagura,[15] A. Balboni,[26] W. Baldini,[26] L. Balzani,[19] H. Bao,[7] J. Baptista de Souza Leite,[61] C. Barbero Pretel,[47,12] M. Barbetti,[27] I. R. Barbosa,[70] R. J. Barlow,[63] M. Barnyakov,[25] S. Barsuk,[14] W. Barter,[59] J. Bartz,[69] S. Bashir,[40] B. Batsukh,[5] P. B. Battista,[14] A. Bay,[50] A. Beck,[65] M. Becker,[19] F. Bedeschi,[35] I. B. Bediaga,[2] N. A. Behling,[19] S. Belin,[47] K. Belous,[44] I. Belov,[29] I. Belyaev,[36] G. Benane,[13] G. Bencivenni,[28] E. Ben-Haim,[16] A. Berezhnoy,[44] R. Bernet,[51] S. Bernet Andres,[46] A. Bertolin,[33] C. Betancourt,[51] F. Betti,[59] J. Bex,[56] Ia. Bezshyiko,[51] O. Bezshyyko,[85] J. Bhom,[41] M. S. Bieker,[18] N. V. Biesuz,[26] P. Billoir,[16] A. Biolchini,[38] M. Birch,[62] F. C. R. Bishop,[10] A. Bitadze,[63] A. Bizzeti, T. Blake,[57] F. Blanc,[50] J. E. Blank,[19] S. Blusk,[69] V. Bocharnikov,[44] J. A. Boelhauve,[19] O. Boente Garcia,[15] T. Boettcher,[68] A. Bohare,[59] A. Boldyrev,[44] C. S. Bolognani,[81] R. Bolzonella,[26] R. B. Bonacci,[1] N. Bondar,[44,49] A. Bordelius,[49] F. Borgato,[33,49] S. Borghi,[63] M. Borsato,[31,c] J. T. Borsuk,[82] E. Bottalico,[61] S. A. Bouchiba,[50] M. Bovill,[64] T. J. V. Bowcock,[61] A. Boyer,[49] C. Bozzi,[26] J. D. Brandenburg,[87] A. Brea Rodriguez,[50] N. Breer,[19] J. Brodzicka,[41] A. Brossa Gonzalo,[47,a] J. Brown,[61] D. Brundu,[32] E. Buchanan,[59] L. Buonincontri,[33,e] M. Burgos Marcos,[81] A. T. Burke,[63] C. Burr,[49] J. S. Butter,[56] J. Buytaert,[49] W. Byczynski,[49] S. Cadeddu,[32] H. Cai,[74] A. Caillet,[16] R. Calabrese,[26,f] S. Calderon Ramirez,[9] L. Calefice,[45] S. Cali,[28] M. Calvi,[31,c] M. Calvo Gomez,[46] P. Camargo Magalhaes,[2,g] J. I. Cambon Bouzas,[47] P. Campana,[28] D. H. Campora Perez,[81] A. F. Campoverde Quezada,[7] S. Capelli,[31] L. Capriotti,[26] R. Caravaca-Mora,[9] A. Carbone,[25,h] L. Carcedo Salgado,[47] R. Cardinale,[29,i] A. Cardini,[32] P. Carniti,[31,c] L. Carus,[22] A. Casais Vidal,[65] R. Caspary,[22] G. Casse,[61] M. Cattaneo,[49] G. Cavallero,[26,49] V. Cavallini,[26,f] S. Celani,[22] S. Cesare,[30,j] A. J. Chadwick,[61] I. Chahrour,[86] H. Chang,[4,k] M. Charles,[16] Ph. Charpentier,[49] E. Chatzianagnostou,[38] M. Chefdeville,[10] C. Chen,[56] S. Chen,[5] Z. Chen,[7] A. Chernov,[41] S. Chernyshenko,[53] X. Chiotopoulos,[81] V. Chobanova,[83] M. Chrzaszcz,[41] A. Chubykin,[44] V. Chulikov,[28,36] P. Ciambrone,[28] X. Cid Vidal,[47] G. Ciezarek,[49] P. Cifra,[49] P. E. L. Clarke,[59] M. Clemencic,[49] H. V. Cliff,[56] J. Closier,[49] C. Cocha Toapaxi,[22] V. Coco,[49] J. Cogan,[13] E. Cogneras,[11] L. Cojocariu,[43] S. Collaviti,[50] P. Collins,[49] T. Colombo,[49] M. Colonna,[19] A. Comerma-Montells,[45] L. Congedo,[24] A. Contu,[32] N. Cooke,[60] C. Coronel,[66] I. Corredoira,[12] A. Correia,[16] G. Corti,[49] J. Cottee Meldrum,[55] B. Couturier,[49] D. C. Craik,[51] M. Cruz Torres,[2,l] E. Curras Rivera,[50] R. Currie,[59] C. L. Da Silva,[68] S. Dadabaev,[44] L. Dai,[71] X. Dai,[4] E. Dall'Occo,[49] J. Dalseno,[83] C. D'Ambrosio,[62] J. Daniel,[11] P. d'Argent,[24] G. Darze,[3] A. Davidson,[57] J. E. Davies,[63] O. De Aguiar Francisco,[63] C. De Angelis,[32,m] F. De Benedetti,[49] J. de Boer,[38] K. De Bruyn,[80] S. De Capua,[63] M. De Cian,[22] U. De Freitas Carneiro Da Graca,[2,n] E. De Lucia,[28] J. M. De Miranda,[2] L. De Paula,[3] M. De Serio,[24,o] P. De Simone,[28] F. De Vellis,[19] J. A. de Vries,[81] F. Debernardis,[24] D. Decamp,[10] S. Dekkers,[1] L. Del Buono,[16] B. Delaney,[65] H.-P. Dembinski,[19] J. Deng,[8] V. Denysenko,[51] O. Deschamps,[11] F. Dettori,[32,m] B. Dey,[78] P. Di Nezza,[28] I. Diachkov,[44] S. Didenko,[44] S. Ding,[69] L. Dittmann,[22] V. Dobishuk,[53] A. D. Docheva,[60] C. Dong,[4,k] A. M. Donohoe,[23] F. Dordei,[32] A. C. dos Reis,[2] A. D. Dowling,[69] W. Duan,[72] P. Duda,[82] M. W. Dudek,[41] L. Dufour,[49] V. Duk,[34] P. Durante,[49] M. M. Duras,[82] J. M. Durham,[68] O. D. Durmus,[78] A. Dziurda,[41] A. Dzyuba,[44] S. Easo,[58] E. Eckstein,[18] U. Egede,[1] A. Egorychev,[44] V. Egorychev,[44] S. Eisenhardt,[59] E. Ejopu,[63] L. Eklund,[84] M. Elashri,[66] J. Ellbracht,[19] S. Ely,[62] A. Ene,[43] J. Eschle,[69] S. Esen,[22] T. Evans,[38] F. Fabiano,[32] S. Faghih,[66] L. N. Falcao,[2] B. Fang,[7] L. Fantini,[34,49,p] M. Faria,[50] K. Farmer,[59] D. Fazzini,[31,c] L. Felkowski,[82] M. Feng,[5,7] M. Feo,[2] A. Fernandez Casani,[48] M. Fernandez Gomez,[47] A. D. Fernez,[67] F. Ferrari,[25,h] F. Ferreira Rodrigues,[3] M. Ferrillo,[51] M. Ferro-Luzzi,[49] S. Filippov,[44] R. A. Fini,[24] M. Fiorini,[26,f] M. Firlej,[40] K. L. Fischer,[64] D. S. Fitzgerald,[86] C. Fitzpatrick,[63]

T. Fiutowski,[40] F. Fleuret,[15] M. Fontana,[25] L. F. Foreman,[63] R. Forty,[49] D. Foulds-Holt,[56] V. Franco Lima,[3] M. Franco Sevilla,[67] M. Frank,[49] E. Franzoso,[26,f] G. Frau,[63] C. Frei,[49] D. A. Friday,[63] J. Fu,[7] Q. Führing,[19,56,b] Y. Fujii,[1] T. Fulghesu,[13] E. Gabriel,[38] G. Galati,[24] M. D. Galati,[38] A. Gallas Torreira,[47] D. Galli,[25,h] S. Gambetta,[59] M. Gandelman,[3] P. Gandini,[30] B. Ganie,[63] H. Gao,[7] R. Gao,[64] T. Q. Gao,[56] Y. Gao,[8] Y. Gao,[6] Y. Gao,[8] L. M. Garcia Martin,[50] P. Garcia Moreno,[45] J. García Pardiñas,[65] P. Gardner,[67] K. G. Garg,[8] L. Garrido,[45] C. Gaspar,[49] A. Gavrikov,[33] L. L. Gerken,[19] E. Gersabeck,[20] M. Gersabeck,[20] T. Gershon,[57] S. Ghizzo,[29,i] Z. Ghorbanimoghaddam,[55] L. Giambastiani,[33,e] F. I. Giasemis,[16,q] V. Gibson,[56] H. K. Giemza,[42] A. L. Gilman,[64] M. Giovannetti,[28] A. Gioventù,[45] L. Girardey,[63,58] C. Giugliano,[26,f] M. A. Giza,[41] F. C. Glaser,[14,22] V. V. Gligorov,[16] C. Göbel,[70] L. Golinka-Bezshyyko,[85] E. Golobardes,[46] D. Golubkov,[44] A. Golutvin,[62,49] S. Gomez Fernandez,[45] W. Gomulka,[40] F. Goncalves Abrantes,[64] M. Goncerz,[41] G. Gong,[4,k] J. A. Gooding,[19] I. V. Gorelov,[44] C. Gotti,[31] E. Govorkova,[65] J. P. Grabowski,[18] L. A. Granado Cardoso,[49] E. Graugés,[45] E. Graverini,[50,r] L. Grazette,[57] G. Graziani, A. T. Grecu,[43] L. M. Greeven,[38] N. A. Grieser,[66] L. Grillo,[60] S. Gromov,[44] C. Gu,[15] M. Guarise,[26] L. Guerry,[11] V. Guliaeva,[44] P. A. Günther,[22] A.-K. Guseinov,[50] E. Gushchin,[44] Y. Guz,[6,49] T. Gys,[49] K. Habermann,[18] T. Hadavizadeh,[1] C. Hadjivasiliou,[67] G. Haefeli,[50] C. Haen,[49] G. Hallett,[57] P. M. Hamilton,[67] J. Hammerich,[61] Q. Han,[33] X. Han,[22,49] S. Hansmann-Menzemer,[22] L. Hao,[7] N. Harnew,[64] T. H. Harris,[1] M. Hartmann,[14] S. Hashmi,[40] J. He,[7,s] F. Hemmer,[49] C. Henderson,[66] R. D. L. Henderson,[1,57] A. M. Hennequin,[49] K. Hennessy,[61] L. Henry,[50] J. Herd,[62] P. Herrero Gascon,[22] J. Heuel,[17] A. Hicheur,[3] G. Hijano Mendizabal,[51] J. Horswill,[63] R. Hou,[8] Y. Hou,[11] N. Howarth,[61] J. Hu,[72] W. Hu,[7] X. Hu,[4,k] W. Hulsbergen,[38] R. J. Hunter,[57] M. Hushchyn,[44] D. Hutchcroft,[61] M. Idzik,[40] D. Ilin,[44] P. Ilten,[66] A. Inglessi,[44] A. Iniukhin,[44] A. Ishteev,[44] K. Ivshin,[44] H. Jage,[17] S. J. Jaimes Elles,[76,49,48] S. Jakobsen,[49] E. Jans,[38] B. K. Jashal,[48] A. Jawahery,[67] V. Jevtic,[19] E. Jiang,[67] X. Jiang,[5,7] Y. Jiang,[7] Y. J. Jiang,[6] M. John,[64] A. John Rubesh Rajan,[23] D. Johnson,[54] C. R. Jones,[56] T. P. Jones,[57] S. Joshi,[42] B. Jost,[49] J. Juan Castella,[56] N. Jurik,[49] I. Juszczak,[41] D. Kaminaris,[50] S. Kandybei,[52] M. Kane,[59] Y. Kang,[4,k] C. Kar,[11] M. Karacson,[49] D. Karpenkov,[44] A. Kauniskangas,[50] J. W. Kautz,[66] M. K. Kazanecki,[41] F. Keizer,[49] M. Kenzie,[56] T. Ketel,[38] B. Khanji,[69] A. Kharisova,[44] S. Kholodenko,[35,49] G. Khreich,[14] T. Kirn,[17] V. S. Kirsebom,[31,c] O. Kitouni,[65] S. Klaver,[39] N. Kleijne,[35,t] K. Klimaszewski,[42] M. R. Kmiec,[42] S. Koliiev,[53] L. Kolk,[19] A. Konoplyannikov,[6] P. Kopciewicz,[49] P. Koppenburg,[38] A. Korchin,[52] M. Korolev,[44] I. Kostiuk,[38] O. Kot,[53] S. Kotriakhova, A. Kozachuk,[44] P. Kravchenko,[44] L. Kravchuk,[44] M. Kreps,[57] P. Krokovny,[44] W. Krupa,[69] W. Krzemien,[42] O. Kshyvanskyi,[53] S. Kubis,[82] M. Kucharczyk,[41] V. Kudryavtsev,[44] E. Kulikova,[44] A. Kupsc,[84] V. Kushnir,[52] B. Kutsenko,[13] I. Kyryllin,[52] D. Lacarrere,[49] P. Laguarta Gonzalez,[45] A. Lai,[32] A. Lampis,[32] D. Lancierini,[62] C. Landesa Gomez,[47] J. J. Lane,[1] G. Lanfranchi,[28] C. Langenbruch,[22] J. Langer,[19] O. Lantwin,[44] T. Latham,[57] F. Lazzari,[35,49,r] C. Lazzeroni,[54] R. Le Gac,[13] H. Lee,[61] R. Lefèvre,[11] A. Leflat,[44] S. Legotin,[44] M. Lehuraux,[57] E. Lemos Cid,[49] O. Leroy,[13] T. Lesiak,[41] E. D. Lesser,[49] B. Leverington,[22] A. Li,[4,k] C. Li,[4] C. Li,[13] H. Li,[72] J. Li,[8] K. Li,[75] L. Li,[63] M. Li,[8] P. Li,[7] P.-R. Li,[73] Q. Li,[5,7] S. Li,[8] T. Li,[71] T. Li,[72] Y. Li,[8] Y. Li,[5] Z. Lian,[4,k] X. Liang,[69] S. Libralon,[48] C. Lin,[7] T. Lin,[58] R. Lindner,[49] H. Linton,[62] V. Lisovskyi,[50] R. Litvinov,[32,49] D. Liu,[8] F. L. Liu,[1] G. Liu,[72] K. Liu,[73] S. Liu,[5,7] W. Liu,[8] Y. Liu,[59] Y. Liu,[73] Y. L. Liu,[62] G. Loachamin Ordonez,[70] A. Lobo Salvia,[45] A. Loi,[32] T. Long,[56] J. H. Lopes,[3] A. Lopez Huertas,[45] S. López Soliño,[47] Q. Lu,[15] C. Lucarelli,[27,u] D. Lucchesi,[33,e] M. Lucio Martinez,[48] Y. Luo,[6] A. Lupato,[33,v] E. Luppi,[26,f] K. Lynch,[23] X.-R. Lyu,[7] G. M. Ma,[4,k] S. Maccolini,[19] F. Machefert,[14] F. Maciuc,[43] B. Mack,[69] I. Mackay,[64] L. M. Mackey,[69] L. R. Madhan Mohan,[56] M. J. Madurai,[54] D. Magdalinski,[38] D. Maisuzenko,[44] J. J. Malczewski,[41] S. Malde,[64] L. Malentacca,[49] A. Malinin,[44] T. Maltsev,[44] G. Manca,[32,m] G. Mancinelli,[13] C. Mancuso,[14] R. Manera Escalero,[45] F. M. Manganella,[37] D. Manuzzi,[25] D. Marangotto,[30] J. F. Marchand,[10] R. Marchevski,[50] U. Marconi,[25] E. Mariani,[16] S. Mariani,[49] C. Marin Benito,[45] J. Marks,[22] A. M. Marshall,[55] L. Martel,[64] G. Martelli,[34,p] G. Martellotti,[36] L. Martinazzoli,[49] M. Martinelli,[31,c] D. Martinez Gomez,[80] D. Martinez Santos,[83] F. Martinez Vidal,[48] A. Martorell i Granollers,[46] A. Massafferri,[2] R. Matev,[49] A. Mathad,[49] V. Matiunin,[44] C. Matteuzzi,[69] K. R. Mattioli,[15] A. Mauri,[62] E. Maurice,[15] J. Mauricio,[45] P. Mayencourt,[50] J. Mazorra de Cos,[48] M. Mazurek,[42] M. McCann,[62] T. H. McGrath,[63] N. T. McHugh,[60] A. McNab,[63] R. McNulty,[23] B. Meadows,[66] G. Meier,[19] D. Melnychuk,[42] F. M. Meng,[4,k] M. Merk,[38,81] A. Merli,[50] L. Meyer Garcia,[67] D. Miao,[5,7] H. Miao,[7] M. Mikhasenko,[77] D. A. Milanes,[76,w]

A. Minotti,[31,c] E. Minucci,[28] T. Miralles,[11] B. Mitreska,[19] D. S. Mitzel,[19] A. Modak,[58] L. Moeser,[19] R. A. Mohammed,[64] R. D. Moise,[17] E. F. Molina Cardenas,[86] T. Mombächer,[49] M. Monk,[57,1] S. Monteil,[11] A. Morcillo Gomez,[47] G. Morello,[28] M. J. Morello,[35,t] M. P. Morgenthaler,[22] J. Moron,[40] W. Morren,[38] A. B. Morris,[49] A. G. Morris,[13] R. Mountain,[69] H. Mu,[4,k] Z. M. Mu,[6] E. Muhammad,[57] F. Muheim,[59] M. Mulder,[80] K. Müller,[51] F. Muñoz-Rojas,[9] R. Murta,[62] V. Mytrochenko,[52] P. Naik,[61] T. Nakada,[50] R. Nandakumar,[58] T. Nanut,[49] I. Nasteva,[3] M. Needham,[59] E. Nekrasova,[44] N. Neri,[30,j] S. Neubert,[18] N. Neufeld,[49] P. Neustroev,[44] J. Nicolini,[49] D. Nicotra,[81] E. M. Niel,[49] N. Nikitin,[44] Q. Niu,[73] P. Nogarolli,[3] P. Nogga,[18] C. Normand,[55] J. Novoa Fernandez,[47] G. Nowak,[66] C. Nunez,[86] H. N. Nur,[60] A. Oblakowska-Mucha,[40] V. Obraztsov,[44] T. Oeser,[17] S. Okamura,[26,f] A. Okhotnikov,[44] O. Okhrimenko,[53] R. Oldeman,[32,m] F. Oliva,[59] M. Olocco,[19] C. J. G. Onderwater,[81] R. H. O'Neil,[49] D. Osthues,[19] J. M. Otalora Goicochea,[3] P. Owen,[51] A. Oyanguren,[48] O. Ozcelik,[59] F. Paciolla,[35,x] A. Padee,[42] K. O. Padeken,[18] B. Pagare,[57] T. Pajero,[49] A. Palano,[24] M. Palutan,[28] X. Pan,[4,k] S. Panebianco,[12] G. Panshin,[5] L. Paolucci,[57] A. Papanestis,[58,49] M. Pappagallo,[24,o] L. L. Pappalardo,[26] C. Pappenheimer,[66] C. Parkes,[63] D. Parmar,[77] B. Passalacqua,[26,f] G. Passaleva,[27] D. Passaro,[35,49,t] A. Pastore,[24] M. Patel,[62] J. Patoc,[64] C. Patrignani,[25,h] A. Paul,[69] C. J. Pawley,[81] A. Pellegrino,[38] J. Peng,[5,7] M. Pepe Altarelli,[28] S. Perazzini,[25] D. Pereima,[44] H. Pereira Da Costa,[68] A. Pereiro Castro,[47] P. Perret,[11] A. Perrevoort,[80] A. Perro,[49,13] M. J. Peters,[66] K. Petridis,[55] A. Petrolini,[29,i] J. P. Pfaller,[66] H. Pham,[69] L. Pica,[35] M. Piccini,[34] L. Piccolo,[32] B. Pietrzyk,[10] G. Pietrzyk,[14] R. N. Pilato,[61] D. Pinci,[36] F. Pisani,[49] M. Pizzichemi,[31,49,c] V. Placinta,[43] M. Plo Casasus,[47] T. Poeschl,[49] F. Polci,[16] M. Poli Lener,[28] A. Poluektov,[13] N. Polukhina,[44] I. Polyakov,[63] E. Polycarpo,[3] S. Ponce,[49] D. Popov,[7,49] S. Poslavskii,[44] K. Prasanth,[59] C. Prouve,[83] D. Provenzano,[32,m] V. Pugatch,[53] G. Punzi,[35,r] S. Qasim,[51] Q. Q. Qian,[6] W. Qian,[7] N. Qin,[4,k] S. Qu,[4,k] R. Quagliani,[49] R. I. Rabadan Trejo,[57] J. H. Rademacker,[55] M. Rama,[35] M. Ramírez García,[86] V. Ramos De Oliveira,[70] M. Ramos Pernas,[57] M. S. Rangel,[3] F. Ratnikov,[44] G. Raven,[39] M. Rebollo De Miguel,[48] F. Redi,[30,v] J. Reich,[55] F. Reiss,[20] Z. Ren,[7] P. K. Resmi,[64] M. Ribalda Galvez,[45] R. Ribatti,[50] G. Ricart,[15,12] D. Riccardi,[35,t] S. Ricciardi,[58] K. Richardson,[65] M. Richardson-Slipper,[59] K. Rinnert,[61] P. Robbe,[14,49] G. Robertson,[60] E. Rodrigues,[61] A. Rodriguez Alvarez,[45] E. Rodriguez Fernandez,[47] J. A. Rodriguez Lopez,[76] E. Rodriguez Rodriguez,[49] J. Roensch,[19] A. Rogachev,[44] A. Rogovskiy,[58] D. L. Rolf,[19] P. Roloff,[49] V. Romanovskiy,[66] A. Romero Vidal,[47] G. Romolini,[26] F. Ronchetti,[50] T. Rong,[6] M. Rotondo,[28] S. R. Roy,[22] M. S. Rudolph,[69] M. Ruiz Diaz,[22] R. A. Ruiz Fernandez,[47] J. Ruiz Vidal,[81] J. J. Saavedra-Arias,[9] J. J. Saborido Silva,[47] R. Sadek,[15] N. Sagidova,[44] D. Sahoo,[78] N. Sahoo,[54] B. Saitta,[32,m] M. Salomoni,[31,49,c] I. Sanderswood,[48] R. Santacesaria,[36] C. Santamarina Rios,[47] M. Santimaria,[28] L. Santoro,[2] E. Santovetti,[37] A. Saputi,[26,49] D. Saranin,[44] A. Sarnatskiy,[80] G. Sarpis,[59] M. Sarpis,[79] C. Satriano,[36,y] A. Satta,[37] M. Saur,[73] D. Savrina,[44] H. Sazak,[17] F. Sborzacchi,[49,28] A. Scarabotto,[19] S. Schael,[17] S. Scherl,[61] M. Schiller,[60] H. Schindler,[49] M. Schmelling,[21] B. Schmidt,[49] S. Schmitt,[17] H. Schmitz,[18] O. Schneider,[50] A. Schopper,[62] N. Schulte,[19] S. Schulte,[50] M. H. Schune,[14] G. Schwering,[17] B. Sciascia,[28] A. Sciuccati,[49] I. Segal,[77] S. Sellam,[47] A. Semennikov,[44] T. Senger,[51] M. Senghi Soares,[39] A. Sergi,[29,i] N. Serra,[51] L. Sestini,[27] A. Seuthe,[19] B. Sevilla Sanjuan,[46] Y. Shang,[6] D. M. Shangase,[86] M. Shapkin,[44] R. S. Sharma,[69] I. Shchemerov,[44] L. Shchutska,[50] T. Shears,[61] L. Shekhtman,[44] Z. Shen,[38] S. Sheng,[5,7] V. Shevchenko,[44] B. Shi,[7] Q. Shi,[7] Y. Shimizu,[14] E. Shmanin,[25] R. Shorkin,[44] J. D. Shupperd,[69] R. Silva Coutinho,[69] G. Simi,[33,e] S. Simone,[24,o] M. Singha,[78] N. Skidmore,[57] T. Skwarnicki,[69] M. W. Slater,[54] E. Smith,[65] K. Smith,[68] M. Smith,[62] L. Soares Lavra,[59] M. D. Sokoloff,[66] F. J. P. Soler,[60] A. Solomin,[55] A. Solovev,[44] I. Solovyev,[44] N. S. Sommerfeld,[18] R. Song,[1] Y. Song,[50] Y. Song,[4,k] Y. S. Song,[6] F. L. Souza De Almeida,[69] B. Souza De Paula,[3] E. Spadaro Norella,[29,i] E. Spedicato,[25] J. G. Speer,[19] E. Spiridenkov,[44] P. Spradlin,[60] V. Sriskaran,[49] F. Stagni,[49] M. Stahl,[77] S. Stahl,[49] S. Stanislaus,[64] M. Stefaniak,[87] E. N. Stein,[49] O. Steinkamp,[51] O. Stenyakin,[44] H. Stevens,[19] D. Strekalina,[44] Y. Su,[7] F. Suljik,[64] J. Sun,[32] L. Sun,[74] D. Sundfeld,[2] W. Sutcliffe,[51] K. Swientek,[40] F. Swystun,[56] A. Szabelski,[42] T. Szumlak,[40] Y. Tan,[4,k] Y. Tang,[74] Y. T. Tang,[7] M. D. Tat,[22] A. Terentev,[44] F. Terzuoli,[35,49,x] F. Teubert,[49] U. Thoma,[18] E. Thomas,[49] D. J. D. Thompson,[54] H. Tilquin,[62] V. Tisserand,[11] S. T'Jampens,[10] M. Tobin,[5] L. Tomassetti,[26,f] G. Tonani,[30,j] X. Tong,[6] T. Tork,[30] D. Torres Machado,[2] L. Toscano,[19] D. Y. Tou,[4,k] C. Trippl,[46] G. Tuci,[22] N. Tuning,[38]

L. H. Uecker,[22] A. Ukleja,[40] D. J. Unverzagt,[22] A. Upadhyay,[78] B. Urbach,[59] A. Usachov,[39] A. Ustyuzhanin,[44] U. Uwer,[22] V. Vagnoni,[25] V. Valcarce Cadenas,[47] G. Valenti,[25] N. Valls Canudas,[49] J. van Eldik,[49] H. Van Hecke,[68] E. van Herwijnen,[62] C. B. Van Hulse,[47,z] R. Van Laak,[50] M. van Veghel,[38] G. Vasquez,[51] R. Vazquez Gomez,[45] P. Vazquez Regueiro,[47] C. Vázquez Sierra,[83] S. Vecchi,[26] J. J. Velthuis,[55] M. Veltri,[27,aa] A. Venkateswaran,[50] M. Verdoglia,[32] M. Vesterinen,[57] D. Vico Benet,[64] P. Vidrier Villalba,[45] M. Vieites Diaz,[47] X. Vilasis-Cardona,[46] E. Vilella Figueras,[61] A. Villa,[25] P. Vincent,[16] B. Vivacqua,[3] F. C. Volle,[54] D. vom Bruch,[13] N. Voropaev,[44] K. Vos,[81] C. Vrahas,[59] J. Wagner,[19] J. Walsh,[35] E. J. Walton,[1,57] G. Wan,[6] A. Wang,[7] C. Wang,[22] G. Wang,[8] H. Wang,[73] J. Wang,[6] J. Wang,[5] J. Wang,[4,k] J. Wang,[74] M. Wang,[49] N. W. Wang,[7] R. Wang,[55] X. Wang,[8] X. Wang,[72] X. W. Wang,[62] Y. Wang,[75] Y. Wang,[6] Y. W. Wang,[73] Z. Wang,[14] Z. Wang,[4,k] Z. Wang,[30] J. A. Ward,[57,1] M. Waterlaat,[49] N. K. Watson,[54] D. Websdale,[62] Y. Wei,[6] J. Wendel,[83] B. D. C. Westhenry,[55] C. White,[56] M. Whitehead,[60] E. Whiter,[54] A. R. Wiederhold,[63] D. Wiedner,[19] G. Wilkinson,[64,49] M. K. Wilkinson,[66] M. Williams,[65] M. J. Williams,[49] M. R. J. Williams,[59] R. Williams,[56] Z. Williams,[55] F. F. Wilson,[58] M. Winn,[12] W. Wislicki,[42] M. Witek,[41] L. Witola,[19] G. Wormser,[14] S. A. Wotton,[56] H. Wu,[69] J. Wu,[8] X. Wu,[74] Y. Wu,[6,56] Z. Wu,[7] K. Wyllie,[49] S. Xian,[72] Z. Xiang,[5] Y. Xie,[8] T. X. Xing,[30] A. Xu,[35] L. Xu,[4,k] L. Xu,[4,k] M. Xu,[57] Z. Xu,[49] Z. Xu,[7] Z. Xu,[5] K. Yang,[62] X. Yang,[6] Y. Yang,[29,i] Z. Yang,[6] V. Yeroshenko,[14] H. Yeung,[63] H. Yin,[8] X. Yin,[7] C. Y. Yu,[6] J. Yu,[71] X. Yuan,[5] Y Yuan,[5,7] E. Zaffaroni,[50] M. Zavertyaev,[21] M. Zdybal,[41] F. Zenesini,[25] C. Zeng,[5,7] M. Zeng,[4,k] C. Zhang,[6] D. Zhang,[8] J. Zhang,[7] L. Zhang,[4,k] R. Zhang,[8] S. Zhang,[71] S. Zhang,[64] Y. Zhang,[6] Y. Z. Zhang,[4,k] Z. Zhang,[4,k] Y. Zhao,[22] A. Zhelezov,[22] S. Z. Zheng,[6] X. Z. Zheng,[4,k] Y. Zheng,[7] T. Zhou,[6] X. Zhou,[8] Y. Zhou,[7] V. Zhovkovska,[57] L. Z. Zhu,[7] X. Zhu,[4,k] X. Zhu,[8] Y. Zhu,[17] V. Zhukov,[17] J. Zhuo,[48] Q. Zou,[5,7] D. Zuliani,[33,e] and G. Zunica[50]

(LHCb Collaboration)

[1]*School of Physics and Astronomy, Monash University, Melbourne, Australia*
[2]*Centro Brasileiro de Pesquisas Físicas (CBPF), Rio de Janeiro, Brazil*
[3]*Universidade Federal do Rio de Janeiro (UFRJ), Rio de Janeiro, Brazil*
[4]*Department of Engineering Physics, Tsinghua University, Beijing, China*
[5]*Institute Of High Energy Physics (IHEP), Beijing, China*
[6]*School of Physics State Key Laboratory of Nuclear Physics and Technology, Peking University, Beijing, China*
[7]*University of Chinese Academy of Sciences, Beijing, China*
[8]*Institute of Particle Physics, Central China Normal University, Wuhan, Hubei, China*
[9]*Consejo Nacional de Rectores (CONARE), San Jose, Costa Rica*
[10]*Université Savoie Mont Blanc, CNRS, IN2P3-LAPP, Annecy, France*
[11]*Université Clermont Auvergne, CNRS/IN2P3, LPC, Clermont-Ferrand, France*
[12]*Université Paris-Saclay, Centre d'Etudes de Saclay (CEA), IRFU, Saclay, France, Gif-Sur-Yvette, France*
[13]*Aix Marseille Univ, CNRS/IN2P3, CPPM, Marseille, France*
[14]*Université Paris-Saclay, CNRS/IN2P3, IJCLab, Orsay, France*
[15]*Laboratoire Leprince-Ringuet, CNRS/IN2P3, Ecole Polytechnique, Institut Polytechnique de Paris, Palaiseau, France*
[16]*LPNHE, Sorbonne Université, Paris Diderot Sorbonne Paris Cité, CNRS/IN2P3, Paris, France*
[17]*I. Physikalisches Institut, RWTH Aachen University, Aachen, Germany*
[18]*Universität Bonn - Helmholtz-Institut für Strahlen und Kernphysik, Bonn, Germany*
[19]*Fakultät Physik, Technische Universität Dortmund, Dortmund, Germany*
[20]*Physikalisches Institut, Albert-Ludwigs-Universität Freiburg, Freiburg, Germany*
[21]*Max-Planck-Institut für Kernphysik (MPIK), Heidelberg, Germany*
[22]*Physikalisches Institut, Ruprecht-Karls-Universität Heidelberg, Heidelberg, Germany*
[23]*School of Physics, University College Dublin, Dublin, Ireland*
[24]*INFN Sezione di Bari, Bari, Italy*
[25]*INFN Sezione di Bologna, Bologna, Italy*
[26]*INFN Sezione di Ferrara, Ferrara, Italy*
[27]*INFN Sezione di Firenze, Firenze, Italy*
[28]*INFN Laboratori Nazionali di Frascati, Frascati, Italy*
[29]*INFN Sezione di Genova, Genova, Italy*
[30]*INFN Sezione di Milano, Milano, Italy*

[31]INFN Sezione di Milano-Bicocca, Milano, Italy
[32]INFN Sezione di Cagliari, Monserrato, Italy
[33]INFN Sezione di Padova, Padova, Italy
[34]INFN Sezione di Perugia, Perugia, Italy
[35]INFN Sezione di Pisa, Pisa, Italy
[36]INFN Sezione di Roma La Sapienza, Roma, Italy
[37]INFN Sezione di Roma Tor Vergata, Roma, Italy
[38]Nikhef National Institute for Subatomic Physics, Amsterdam, Netherlands
[39]Nikhef National Institute for Subatomic Physics and VU University Amsterdam, Amsterdam, Netherlands
[40]AGH - University of Krakow, Faculty of Physics and Applied Computer Science, Kraków, Poland
[41]Henryk Niewodniczanski Institute of Nuclear Physics Polish Academy of Sciences, Kraków, Poland
[42]National Center for Nuclear Research (NCBJ), Warsaw, Poland
[43]Horia Hulubei National Institute of Physics and Nuclear Engineering, Bucharest-Magurele, Romania
[44]Authors affiliated with an institute formerly covered by a cooperation agreement with CERN
[45]ICCUB, Universitat de Barcelona, Barcelona, Spain
[46]La Salle, Universitat Ramon Llull, Barcelona, Spain
[47]Instituto Galego de Física de Altas Enerxías (IGFAE), Universidade de Santiago de Compostela, Santiago de Compostela, Spain
[48]Instituto de Fisica Corpuscular, Centro Mixto Universidad de Valencia - CSIC, Valencia, Spain
[49]European Organization for Nuclear Research (CERN), Geneva, Switzerland
[50]Institute of Physics, Ecole Polytechnique Fédérale de Lausanne (EPFL), Lausanne, Switzerland
[51]Physik-Institut, Universität Zürich, Zürich, Switzerland
[52]NSC Kharkiv Institute of Physics and Technology (NSC KIPT), Kharkiv, Ukraine
[53]Institute for Nuclear Research of the National Academy of Sciences (KINR), Kyiv, Ukraine
[54]School of Physics and Astronomy, University of Birmingham, Birmingham, United Kingdom
[55]H.H. Wills Physics Laboratory, University of Bristol, Bristol, United Kingdom
[56]Cavendish Laboratory, University of Cambridge, Cambridge, United Kingdom
[57]Department of Physics, University of Warwick, Coventry, United Kingdom
[58]STFC Rutherford Appleton Laboratory, Didcot, United Kingdom
[59]School of Physics and Astronomy, University of Edinburgh, Edinburgh, United Kingdom
[60]School of Physics and Astronomy, University of Glasgow, Glasgow, United Kingdom
[61]Oliver Lodge Laboratory, University of Liverpool, Liverpool, United Kingdom
[62]Imperial College London, London, United Kingdom
[63]Department of Physics and Astronomy, University of Manchester, Manchester, United Kingdom
[64]Department of Physics, University of Oxford, Oxford, United Kingdom
[65]Massachusetts Institute of Technology, Cambridge, Massachusetts, USA
[66]University of Cincinnati, Cincinnati, Ohio, USA
[67]University of Maryland, College Park, Maryland, USA
[68]Los Alamos National Laboratory (LANL), Los Alamos, New Mexico, USA
[69]Syracuse University, Syracuse, New York, USA
[70]Pontifícia Universidade Católica do Rio de Janeiro (PUC-Rio), Rio de Janeiro, Brazil
(associated with Universidade Federal do Rio de Janeiro (UFRJ), Rio de Janeiro, Brazil)
[71]School of Physics and Electronics, Hunan University, Changsha City, China
(associated with Institute of Particle Physics, Central China Normal University, Wuhan, Hubei, China)
[72]Guangdong Provincial Key Laboratory of Nuclear Science, Guangdong-Hong Kong Joint Laboratory of Quantum Matter, Institute of Quantum Matter, South China Normal University, Guangzhou, China
(associated with Department of Engineering Physics, Tsinghua University, Beijing, China)
[73]Lanzhou University, Lanzhou, China
(associated with Institute Of High Energy Physics (IHEP), Beijing, China)
[74]School of Physics and Technology, Wuhan University, Wuhan, China
(associated with Department of Engineering Physics, Tsinghua University, Beijing, China)
[75]Henan Normal University, Xinxiang, China
(associated with Institute of Particle Physics, Central China Normal University, Wuhan, Hubei, China)
[76]Departamento de Fisica, Universidad Nacional de Colombia, Bogota, Colombia
(associated with LPNHE, Sorbonne Université, Paris Diderot Sorbonne Paris Cité, CNRS/IN2P3, Paris, France)
[77]Ruhr Universitaet Bochum, Fakultaet f. Physik und Astronomie, Bochum, Germany
(associated with Fakultät Physik, Technische Universität Dortmund, Dortmund, Germany)
[78]Eotvos Lorand University, Budapest, Hungary
(associated with European Organization for Nuclear Research (CERN), Geneva, Switzerland)
[79]Faculty of Physics, Vilnius University, Vilnius, Lithuania
(associated with Physikalisches Institut, Albert-Ludwigs-Universität Freiburg, Freiburg, Germany)

[80]Van Swinderen Institute, University of Groningen, Groningen, Netherlands
(associated with Nikhef National Institute for Subatomic Physics, Amsterdam, Netherlands)
[81]Universiteit Maastricht, Maastricht, Netherlands
(associated with Nikhef National Institute for Subatomic Physics, Amsterdam, Netherlands)
[82]Tadeusz Kosciuszko Cracow University of Technology, Cracow, Poland
(associated with Henryk Niewodniczanski Institute of Nuclear Physics Polish Academy of Sciences, Kraków, Poland)
[83]Universidade da Coruña, A Coruña, Spain
(associated with La Salle, Universitat Ramon Llull, Barcelona, Spain)
[84]Department of Physics and Astronomy, Uppsala University, Uppsala, Sweden
(associated with School of Physics and Astronomy, University of Glasgow, Glasgow, United Kingdom)
[85]Taras Schevchenko University of Kyiv, Faculty of Physics, Kyiv, Ukraine
(associated with Université Paris-Saclay, CNRS/IN2P3, IJCLab, Orsay, France)
[86]University of Michigan, Ann Arbor, Michigan, USA
(associated with Syracuse University, Syracuse, New York, USA)
[87]Ohio State University, Columbus, USA
(associated with Los Alamos National Laboratory (LANL), Los Alamos, New Mexico, USA)

[a]Deceased.
[b]Also at Lamarr Institute for Machine Learning and Artificial Intelligence, Dortmund, Germany.
[c]Also at Università degli Studi di Milano-Bicocca, Milano, Italy.
[d]Also at Università di Roma Tor Vergata, Roma, Italy.
[e]Also at Università di Padova, Padova, Italy.
[f]Also at Università di Ferrara, Ferrara, Italy.
[g]Also at Facultad de Ciencias Fisicas, Madrid, Spain.
[h]Also at Università di Bologna, Bologna, Italy.
[i]Also at Università di Genova, Genova, Italy.
[j]Also at Università degli Studi di Milano, Milano, Italy.
[k]Also at Center for High Energy Physics, Tsinghua University, Beijing, China.
[l]Also at Universidad Nacional Autónoma de Honduras, Tegucigalpa, Honduras.
[m]Also at Università di Cagliari, Cagliari, Italy.
[n]Also at Centro Federal de Educacão Tecnológica Celso Suckow da Fonseca, Rio De Janeiro, Brazil.
[o]Also at Università di Bari, Bari, Italy.
[p]Also at Università di Perugia, Perugia, Italy.
[q]Also at LIP6, Sorbonne Université, Paris, France.
[r]Also at Università di Pisa, Pisa, Italy.
[s]Also at Hangzhou Institute for Advanced Study, UCAS, Hangzhou, China.
[t]Also at Scuola Normale Superiore, Pisa, Italy.
[u]Also at Università di Firenze, Firenze, Italy.
[v]Also at Università di Bergamo, Bergamo, Italy.
[w]Also at Universidad de Ingeniería y Tecnología (UTEC), Lima, Peru.
[x]Also at Università di Siena, Siena, Italy.
[y]Also at Università della Basilicata, Potenza, Italy.
[z]Also at Universidad de Alcalá, Alcalá de Henares, Spain.
[aa]Also at Università di Urbino, Urbino, Italy.